Advancing the Accuracy of Computational Models for Double-Sided Incremental Forming

Newell Moser [a,] ***, Dohyun Leem** [b], **Shuheng Liao** [b], **Kornel Ehmann** [b], **Jian Cao** [b]

[a] National Institute of Standards and Technology, Applied Chemicals and Materials Division, 325 Broadway, Boulder, CO, 80305, USA
[b] Northwestern University, Department of Mechanical Engineering, 2145 Sheridan Rd, Evanston, IL, 60201, USA
***** Corresponding author, Phone: +1 (303) 497-5711, Email: newell.moser@nist.gov

Newell Moser: newell.moser@nist.gov
Dohyun Leem: dohyunleem2021@u.northwestern.edu
Shuheng Liao: shuhengliao2023@u.northwestern.edu
Kornel Ehmann: k-ehmann@northwestern.edu
Jian Cao: jcao@northwestern.edu

Abstract

Double-Sided Incremental Forming (DSIF) is a rapid-prototyping manufacturing process for metal forming that, for low-volume production, is competitively energy-efficient. However, controlling the DSIF process in terms of accuracy and formability is an ongoing challenge. These control challenges arise due to a lack of understanding of the underlying deformation mechanisms in DSIF, which finite element simulations can help to unravel. However, DSIF pushes the limits of modern finite element formulations due to true strains that approach one, finite rotations, nonlinear contact, and triaxial stress states that range across multiple length scales. To confidently develop a finite element model of DSIF, an extensive verification process must be considered, which is the objective of this study. In this work, different finite element types and varying amounts of artificial acceleration are investigated, and recommendations based on efficiency and accuracy are summarized. A simplified, axisymmetric geometry was considered to reduce simulation time. For this geometry, accelerating the explicit finite element simulation by a mass factor of 10^5 or greater affected the stress triaxiality in the sheet by as much as 40% in some locations with respect to the quasi-static case. Additionally, the ratio of the kinetic energy to internal energy of the sheet was not a reliable indicator of whether a DSIF simulation is approximately quasi-static.

Keywords

Metal forming, Simulation, Finite element, Verification, Mass scaling

1. Introduction and Motivation

Double-Sided Incremental Forming (DSIF) is a flexible metal forming process that uses two numerically controlled tools – one above and one below the sheet – that move along a predefined toolpath [1]. In addition to flexibility, parts formed by DSIF demonstrate a marked improvement in formability relative to conventional forming processes like stamping [2]. More specifically, failure strains in DSIF surpass those observed in stamping, which are usually defined by the necking limit and are characterized by forming limit diagrams.

Although DSIF has great potential towards the rapid production of freeform sheet metal parts, the use of a secondary tool also contributes to additional challenges that can affect process control. Similar to Single-Point Incremental Forming (SPIF), the principal technical challenges in DSIF are related to process control: geometric accuracy, surface quality, process throughput, and excessive thinning or fracture [3]. In order to improve process control, there is a need to develop accurate, efficient models of DSIF in order to better understand the mechanics of the process, as well as to quantify values which cannot be easily measured (e.g., residual stresses).

There are numerous challenges associated with simulating DSIF. Even forming a simple geometry, like a funnel, involves large-strain deformations, finite rotations, cyclic loading-unloading histories, nonlinear material behavior, contact-impact interfaces, and a range of triaxial stress states. To overcome these challenging nonlinearities, state-of-the-art techniques within the finite element method are commonly used [4–7].

Without any artificial acceleration, a finite element simulation of DSIF could readily require *months* to finish [8]. One strategy to speed up a simulation is to choose a simpler geometry, like an axisymmetric part, and develop a reduced model [7]. Though, for large finite element problems, explicit (transient) integrators with artificial acceleration tend to scale better than implicit (equilibrium) integrators, particularly if strong nonlinearities are present like contact interfaces. For a more detailed discussion on explicit and implicit finite element methods, the interested reader is referred to Belytschko et al. [9] and Wriggers [10]. Since full-scale simulations of DSIF often involve a large number of finite elements (greater than 10^6 degrees of freedom), explicit methods are a popular choice to model the process [6, 11].

To artificially accelerate an explicit finite element model, either mass scaling or velocity scaling can be used. By increasing the mass in the model, the stable time step associated with explicit simulations increases, thereby necessitating fewer time steps to complete the simulation. Researchers simulating incremental sheet forming commonly use a mass scaling factor of 10^5, or more [6, 11, 12]. On the other hand, researchers must be careful not to use too much artificial acceleration. Otherwise, the model will no longer be a fair approximation of the real process, which is usually quasi-static depending on the tool speed. However, for a given DSIF model, it is currently unclear what a safe upper limit is in terms of mass scaling.

In this study, we develop a simplified finite element model of DSIF in order to verify the relative effects of varying key parameters in the model. By changing the parameters in the model, like mass scaling, the predicted stresses and strains will be shown to significantly change relative to the baseline quasi-static simulation. As a result, recommended values and methods related to mass scaling and finite element type are given and discussed.

2. Verification Model of DSIF

In order to vary a wide range of finite element parameters within a practical time span, a simplified DSIF model was created which is still capable of capturing the predominant forming mechanics of DSIF. As shown in Figure 1, an axisymmetric, partially-preformed part was chosen, and only half of the model was meshed by using a symmetry boundary condition. In DSIF, shear distortion occurs tangential to the toolpath, so a 10 mm extension was created to distance any erroneous effects of the symmetry boundary condition from the conical region of interest. Although the symmetric boundary condition is not strictly true in DSIF, it is assumed to be a fair assumption since the region of interest is far away from the boundary and the dominant mechanics of DSIF are highly localized. To clarify, the region of interest is within the center of the toolpath's arc just as the tool crosses the X-axis.

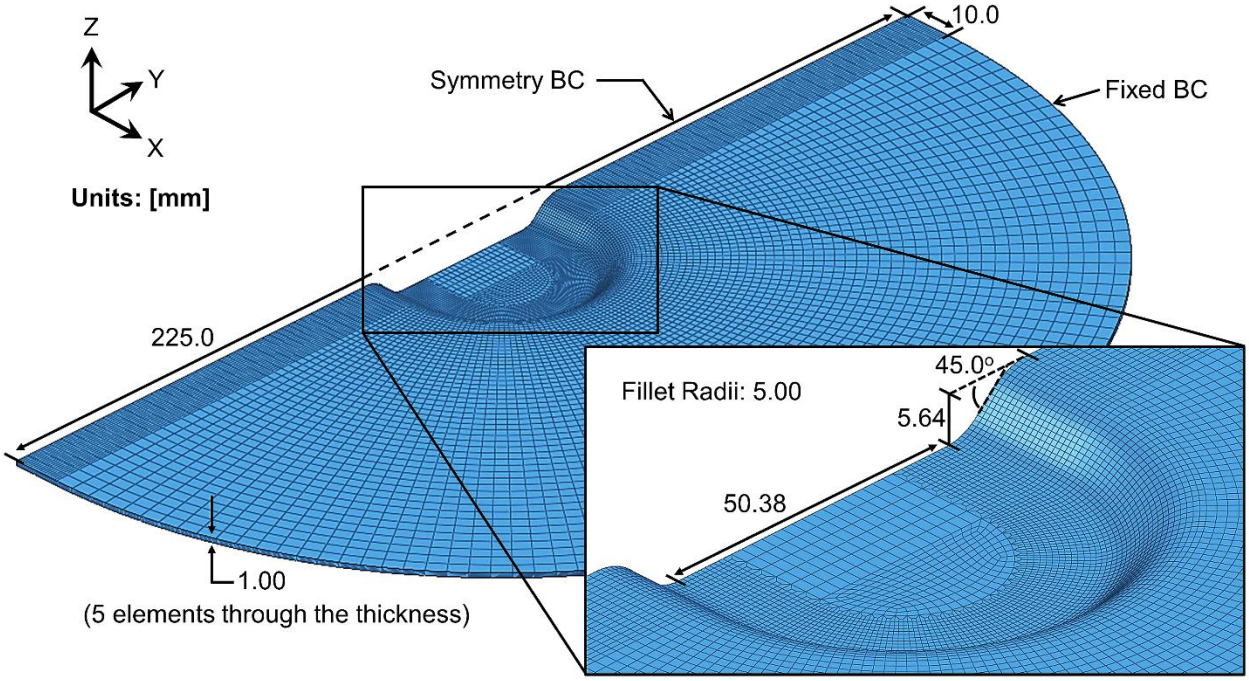

Figure 1. Shown is the finite element mesh used for the verification DSIF model.

For each revolution in the spiral toolpath, a "jump" has been added so that the tools lift-off and then regain contact while traversing along the symmetry boundary condition. By reducing the domain size and performing only five toolpath revolutions for a total length of 731 mm, this simplified model serves as an efficient testbed for comparing finite element procedures in DSIF. However, the proposed verification model is only suggested for investigating *relative* comparisons between simulations.

A total of 55,096 reduced-integration, linear brick elements with stiffness-based hourglass controls [13] were used to model the sheet in Figure 1, while the hemispherical tools – 10 mm in diameter – were modeled with rigid shell elements. Although reduced-integration elements were ultimately chosen, other element formulations were trialed, which will be discussed in the next section. In the forming region, elements were approximately 0.5 mm × 0.5 mm × 0.2 mm in

size. A node-to-surface contact constraint was enforced using the penalty formulation, and friction was neglected. The material of the sheet was modeled after aluminum alloy 5754-O using J_2 flow theory, also commonly referred to as von Mises plasticity with isotropic hardening. A Voce strain hardening model was used within the material model, based on the same parameters used by Moser et al. [4].

All of the verification simulations were performed using Abaqus FEA[1] (version 2017). Since this verification model is simplified and less costly in computational resources than a full-scale model of DSIF, it was reasonable to solve this representative DSIF problem using an implicit (equilibrium) scheme. This static case was used to establish a baseline. Then, the verification model was solved using an explicit (transient) scheme with successive increases in artificial acceleration.

3. Finite Element Type

Different hexahedral element technologies were trialed using the verification model shown in Figure 1 while assuming static conditions. Shell element formulations were not considered in this work due to the underlying assumptions in shell elements related to stresses and strains in the thickness direction, which can be inaccurate for double-sided contact [14]. A summary of the key findings is given in Table 1. Abaqus nomenclature is used as shorthand for the different types of elements: C3D20R is a 20-node, second-order serendipity element that uses reduced integration and stiffness-based hourglass controls; C3D8 is an 8-node, first-order element based on a selectively reduced integration scheme; C3D8I is an 8-node, first order, fully-integrated element that is enhanced by incompatible modes; and C3D8R is an 8-node, reduced-integration element that utilizes stiffness-based hourglass controls. In an effort to be comprehensive, shear locking, volumetric locking, and hourglass controls are briefly summarized next; more details are discussed by Belytschko et al. [9].

Shear locking occurs in first-order, fully-integrated elements that are subjected to bending. The numerical formulation of these elements gives rise to shear strains that do not really exist – the so-called parasitic shear. Therefore, these elements are too stiff in bending. Volumetric locking (sometimes termed pressure locking) occurs in fully-integrated elements when the material behavior is incompressible, such as von Mises materials. Spurious pressure-stresses develop at the integration points, causing an element to behave too stiffly for deformations that should cause no volume changes (see Figure 2). Reduced-integration, or under-integrated, refers to using fewer Gaussian integration points than are necessary to integrate the element matrices exactly for an undistorted element. A linear (i.e., first-order) element with reduced-integration implies that a single integration point is used, which is located at the element center.

[1] Certain commercial equipment, software and/or materials are identified in this paper in order to adequately specify the experimental or simulation procedure. In no case does such identification imply recommendation or endorsement by the National Institute of Standards and Technology, nor does it imply that the equipment and/or materials used are necessarily the best available for the purpose.

Table 1. Results of trialing different solid continuum elements in the verification DSIF model. Wall time is defined as the elapsed "wall-clock" time required to complete the simulation. HG is short for hourglass, and SR for selectively reduced.

Type of Hexahedral Solid Continuum Element	Shear Locking	Volumetric Locking	Wall Time × Number of Computer Cores (CPU · hr)
C3D20R (w/ HG Controls)	Minimal	Severe	(256.3 hr) × (72 CPU) = 18,454
C3D8 (SR Integration)	Severe	None	(52.5 hr) × (24 CPU) = 1,260
C3D8I (Incompatible Modes)	Severe	Moderate	(86.2 hr) × (24 CPU) = 2,069
C3D8R (w/ HG Controls)	None	None	(60.2 hr) × (24 CPU) = 1,446

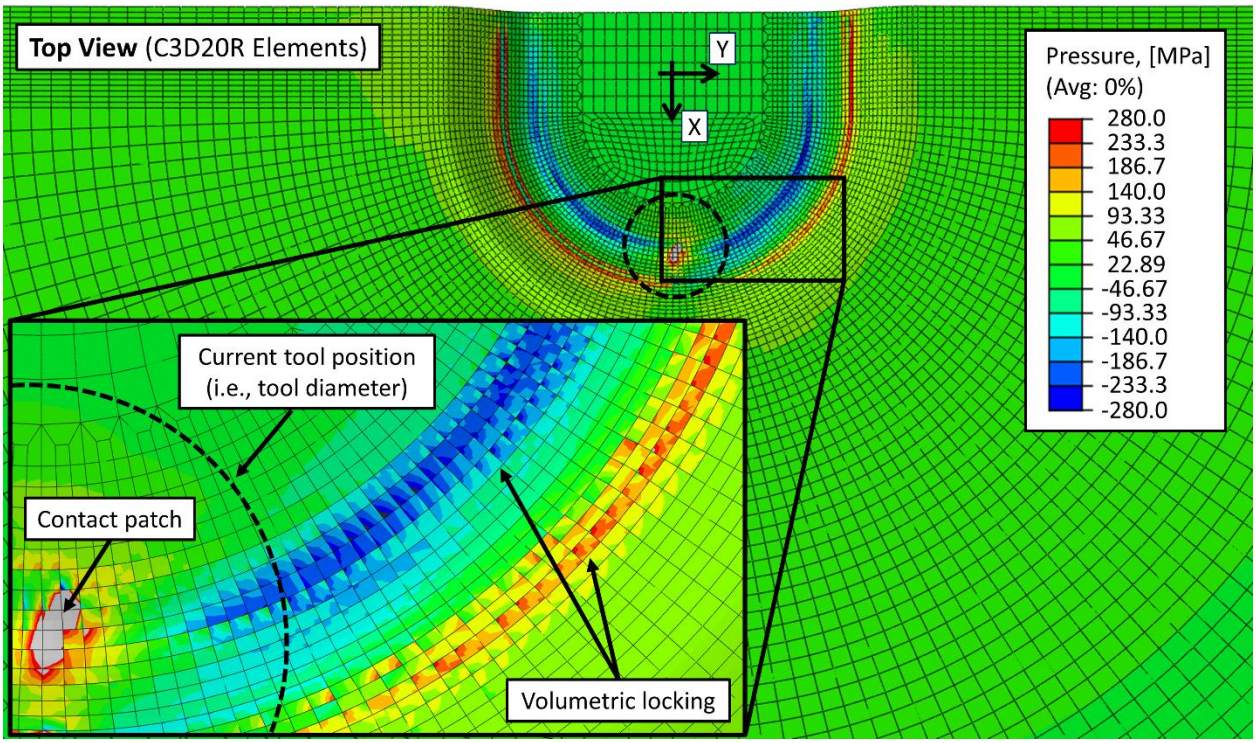

Figure 2. An example of volumetric locking in the pressure (i.e., negative mean stress) field when using quadratic C3D20R elements. Notice the strong discontinuities across element edges. The top and bottom tools (currently hidden) are traversing counterclockwise.

Referring to Table 1, fully-integrated hexahedral elements (C3D9I) fall victim to volumetric locking and shear locking. However, a reduced-integration (or selectively reduced-integration) scheme for the element stiffness matrix not only greatly reduces running time, but these formulations can also alleviate volumetric locking and shear locking. Though, under-integrated elements can result in spurious zero-energy modes of deformation, which are commonly termed "hourglass" modes. Thus, hourglass controls must be employed to artificially stiffen the response of the element against these zero-energy deformation modes. Moreover, hexahedral elements usually provide a solution of equivalent accuracy at less cost compared to tetrahedral elements [9]. However, hexahedral elements are more sensitive to severe mesh distortions, so a structured mesh should be used wherever possible. For these reasons, the C3D8R element with a structured mesh was chosen for this simplified DSIF model.

4. Effects of Mass Scaling

An explicit finite element simulation can be sped up by artificially increasing the mass or scaling the velocity of moving entities. More specifically, increasing the velocity by a factor of k reduces the simulation time by a factor of k, but also artificially increases the kinetic energy by k^2. Increasing the mass (or density) by a factor of k reduces the simulation time by $\sqrt{k}$, but artificially increases the kinetic energy by k. For a given artificial increase in kinetic energy, the effects of accelerating the simplified DSIF model will be similar whether it is achieved through mass or velocity scaling. So, only mass scaling is discussed here.

Referring to Table 2, four cases were considered in evaluating the effects of mass scaling: 1) the Implicit Static case based on solving the static equations using an implicit load-stepping algorithm, 2) the Quasi-Static case based on no mass scaling, 3) the Mass-1 case based on a mass-scaling factor of 1.0×10^3, and 4) the Mass-2 case based on a mass-scaling factor of 1.0×10^5. The tool velocity was set to be constant for all cases involving mass scaling.

Table 2. Mass scaling factors considered in the verification DSIF model. Except for the Implicit Static model, all models utilize an explicit time-stepping algorithm.

Nickname	**Implicit Static**	**Quasi-Static**	**Mass-1**	**Mass-2**
Mass Scaling Factor	1.0	1.0	1.0×10^3	1.0×10^5
Tool Velocity	~	250 mm/s	250 mm/s	250 mm/s
Wall Time (72 cores)	20.1 hr	256.5 hr	8.7 hr	0.9 hr

The stress triaxiality through the thickness during the final toolpath revolution is shown in Figure 3 for each simulation case. Note, the stress triaxiality is defined as the hydrostatic stress divided by the von Mises equivalent stress. With mass scaling, the stress triaxiality lessens in magnitude (becomes more compressive) near regions of contact. More specifically, adding mass by a factor of 10^5 changed the stress triaxiality by 41% near the tip of the top tool, and by 23% near the bottom tool. Mass-1 utilized a moderate amount of mass scaling, and the trends and magnitudes in the stress triaxiality are not significantly altered relative to the Quasi-Static case. Although not shown here, increasing amounts of mass scaling had less of an effect on kinematic quantities – like the equivalent plastic strain – compared to kinetic quantities, like the stress triaxiality and the Lode angle parameter.

Another interesting observation to take note of in Figure 3 is that the Quasi-Static case, based on explicit time-stepping, predicts higher stress triaxialities compared to the Implicit Static case; ideally, they should closely match. We believe these differences are largely due to the numerical implementations of the explicit and implicit procedures, and not because of the physics of the problem at hand. The largest differences in the predictions occurred near regions of contact, which supports the assumption that these effects could be due to the difference in the implementation of the implicit and explicit contact algorithms. Both the implicit scheme (dependent on the iterative Newton's method) and the explicit scheme (based on the central difference method) are second-order accurate in time regarding the truncation error [9]. However, the iterative Newton scheme inherent to implicit methods requires that the energy and displacement residual errors be within a specified tolerance in order to meet convergence

requirements. Explicit methods, on the other hand, do not directly enforce the energy balance; they take a small step forward in time without the need for iterations. Furthermore, explicit methods rely on lumping (i.e., diagonalizing) the mass matrix rather than using the consistent mass matrix, and the lumping procedure is generally performed in an *ad hoc* fashion [15]. Although we can speculate why these differences in the stress triaxialities are appearing, we cannot be certain which is more accurate since this study is limited to relative comparisons. Still, it is interesting to note that, with everything else being equal, the implicit and explicit schemes predicted different magnitudes in the stress triaxialities; though, they do predict similar trends.

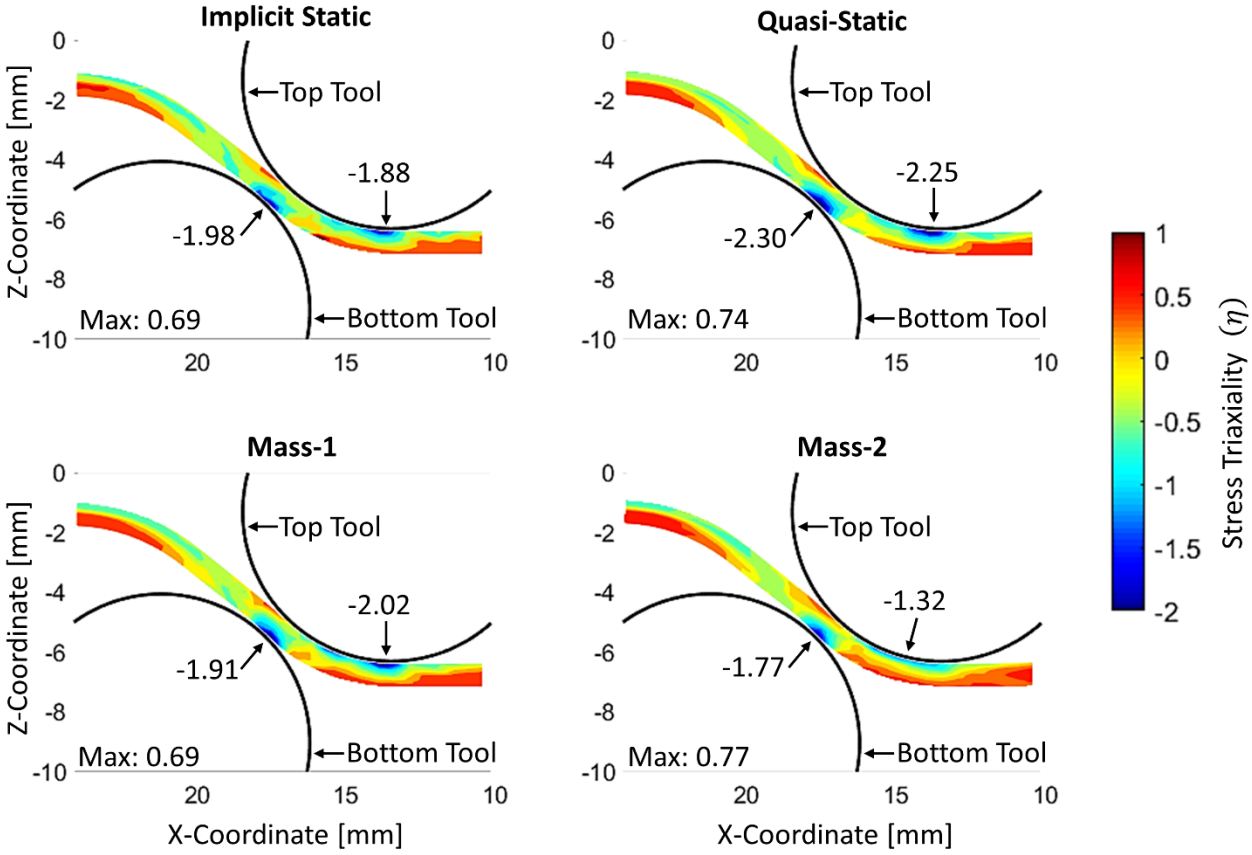

Figure 3. The relative effects of mass scaling on the stress triaxiality. Shown in each case is the cross-sectional side view of the sheet while the tools pass over the X-axis (see Figure 2). The black partial circles represent the perimeter of the tools at this time in the simulation. The minimum (i.e., most compressive) stress triaxialities are pointed out near the regions of contact.

The average forming forces and their corresponding standard deviations are given in Table 3. Although the average magnitudes of the forming forces vary due to mass scaling, the results do not exhibit strong trends. This suggest that increasing the amount of artificial acceleration does not consistently change the average magnitude of the forming forces. On the other hand, increasing the amount of artificial acceleration does result in larger standard deviations of the predicted contact forces. Since the Mass-2 case is not quasi-static based on the changes in the mechanics, as shown in Figure 3, the average forming force is not a good indicator of whether a DSIF simulation is quasi-static or not.

Table 3. The Z-forces (i.e., axial forces) in the top tool are compared between the verification simulations. The average (Avg.) and standard deviation (Std. Dev.) values are calculated from the force histories throughout the final toolpath revolution.

Simulation Case	Avg. Z-Force (N)	Std. Dev. Z-Force (N)
Implicit Static	471.0	$\pm$ 40.9
Quasi-Static	606.1	$\pm$ 30.4
Mass-1	551.5	$\pm$ 63.0
Mass-2	608.6	$\pm$ 89.2

The likely reason that the average forming forces do not significantly differ in Table 3 is because the overall summation of the contact pressures do not significantly change with additional inertial effects. Even though the magnitude of the (compressive) stress triaxialities do change, the total compressive area also changes in such a way to make up for this. Then, when the contact stresses are integrated over the area to calculate the contact forces, the average resultant forces will not change significantly.

One way to determine if a metal forming simulation is quasi-static is to analyze the ratio between the kinetic energy and the internal energy of the deforming metal. In sheet metal forming, the internal energy is usually dominated by the accumulation of plastic strains. If the kinetic energy approaches the internal energy in magnitude, then the deforming sheet is no longer quasi-static. This rule-of-thumb is a reasonable assumption when the entire sheet is deforming, but it does not hold well for DSIF (see Table 4). In DSIF, the localized zones of the sheet will deform as the tools travel along the toolpath, and in effect, the (global) internal energy of the sheet continues to increase over time as new locations experience plastic straining. However, the kinetic energy remains approximately constant over time. Notice in Table 4 that the kinetic energy is at least an order of magnitude less than the internal energy for all cases. However, as stated before, the Mass-2 case is not quasi-static based on Figure 3.

Table 4. The internal energy (I.E.), kinetic energy (K.E.), standard deviation (Std. Dev.) in the kinetic energy of the deformable sheet are compared during the final toolpath revolution. All energy units are in, N·mm.

Simulation Case	Sheet I.E.	Sheet K.E.	Std. Dev. in K.E.
Implicit Static	1.11×10^4	0.00	$\pm$ 0.00
Quasi-Static	1.25×10^4	0.111	$\pm$ 0.088
Mass-1	1.36×10^4	22.4	$\pm$ 10.6
Mass-2	1.54×10^4	366	$\pm$ 118

5. Conclusions and Recommendations

The result of this verification study is a set of finite element parameters that strike a balance between computational efficiency and (relative) accuracy. The following recommendations can be considered for new, full-scale simulations of DSIF. Though, this study is not extensive; there are additional finite element parameters, like the material model, that should be validated in any

new finite element model. Moreover, it is important to recall that a simplified geometry was chosen for this verification study, and consequently, we cannot guarantee that the following conclusions can be extended for all possible toolpaths in DSIF. Rather, these conclusions and recommendations should be considered as reasonable starting points, but further investigating may be necessary for specific geometries. Our conclusions and recommendations are as follows:

- As a starting point for new DSIF models, we recommend scaling the mass between a factor of 10^2 and 10^4, and in general, not above 10^5. Depending on the toolpath and mesh, adding more artificial acceleration can degrade the accuracy of the solution, specifically for kinetic terms like the stress triaxiality and Lode angle parameter.
- In choosing an element type, first-order solid continuum hexahedral elements with reduced-integration and hourglass controls are recommended. They are robust at handling the many sources of nonlinearity that arise in DSIF. However, for improved accuracy, it is important to create a structured mesh that limits element distortion at finite strains. Also, more studies using different finite element technologies should be explored, such as B-bar formulations [16] and hexahedral thick-shell elements.
- The ratio between the global internal energy and global kinetic energy of the sheet should not be used to determine whether a simulation of DSIF is quasi-static. This energy ratio is not applicable because the nature of DSIF involves highly localized deformations. Moreover, the average contact forces are also not a good indicator of whether a DSIF simulation is quasi-static. In future work, it would be worthwhile to formulate a local energy ratio by defining a characteristic length, which could be based on the area of the contact patch between the tools and the sheet. For now, the surest method of evaluating the effects of artificial acceleration is to directly examine the changes in the mechanics, such as the stress triaxiality and Lode angle parameter.

6. References

1. Moser N, Zhang Z, Ren H, Zhang H, Shi Y, Ndip-Agbor EE, Lu B, Chen J, Ehmann KF, Cao J (2016) Effective forming strategy for double-sided incremental forming considering in-plane curvature and tool direction. CIRP Ann - Manuf Technol 65:265–268. https://doi.org/10.1016/j.cirp.2016.04.131
2. Lu B, Fang Y, Xu DK, Chen J, Ai S, Long H, Ou H, Cao J (2015) Investigation of material deformation mechanism in double side incremental sheet forming. Int J Mach Tools Manuf 93:37–48. https://doi.org/10.1016/j.ijmachtools.2015.03.007
3. Li Y, Chen X, Liu Z, Sun J, Li F, Li J, Zhao G (2017) A review on the recent development of incremental sheet-forming process. Int J Adv Manuf Technol 92:2439–2462. https://doi.org/10.1007/s00170-017-0251-z
4. Moser N, Pritchet D, Ren H, Ehmann KF, Cao J (2016) An efficient and general finite element model for double-sided incremental forming. J Manuf Sci Eng 138: https://doi.org/10.1115/1.4033483
5. Smith J, Malhotra R, Liu WK, Cao J (2013) Deformation mechanics in single-point and accumulative double-sided incremental forming. Int J Adv Manuf Technol 69:1185–1201. https://doi.org/10.1007/s00170-013-5053-3

6. Esmaeilpour R, Kim H, Park T, Pourboghrat F, Mohammed B (2017) Comparison of 3D yield functions for finite element simulation of single point incremental forming (SPIF) of aluminum 7075. Int J Mech Sci 133:544–554. https://doi.org/10.1016/j.ijmecsci.2017.09.019
7. Henrard C, Bouffioux C, Eyckens P, Sol H, Duflou JR, Van Houtte P, Van Bael A, Duchêne L, Habraken AM (2011) Forming forces in single point incremental forming: Prediction by finite element simulations, validation and sensitivity. Comput Mech 47:573–590. https://doi.org/10.1007/s00466-010-0563-4
8. Ren H, Moser N, Zhang Z, Ndip-Agbor E, Smith J, Ehmann KF, Cao J (2015) Effects of tool positions in accumulated double-sided incremental forming on part geometry. J Manuf Sci Eng Trans ASME 137:1–8. https://doi.org/10.1115/1.4030528
9. Belytschko T, Liu WK, Moran B, Elkhodary K (2014) Nonlinear Finite Elements for Continua and Structures, 2nd ed. Wiley
10. Wriggers P (2008) Nonlinear Finite Element Methods. Springer-Verlag Berlin Heidelberg
11. Malhotra R, Xue L, Belytschko T, Cao J (2012) Mechanics of fracture in single point incremental forming. J Mater Process Technol 212:1573–1590. https://doi.org/10.1016/j.jmatprotec.2012.02.021
12. Shin J, Bansal A, Nath M, Cheng R, Banu M, Taub A, Martinek B (2018) Prediction of Negative Bulge in Two Point Incremental Forming of an Asymmetric Shape Part. J Phys Conf Ser 1063:012057. https://doi.org/10.1088/1742-6596/1063/1/012057
13. Flanagan DP, Belytschko T (1981) A Uniform Strain Hexahedron and Quadrilateral with Orthogonal Hourglass Control. Int J Numer Methods Eng 17:679–706. https://doi.org/10.1002/nme.1620170504
14. Lee PS, Bathe KJ (2005) Insight into finite element shell discretizations by use of the "basic shell mathematical model." Comput Struct 83:69–90. https://doi.org/10.1016/j.compstruc.2004.07.005
15. Tekkaya AE (2000) State-of-the-art of simulation of sheet metal forming. J Mater Process Technol 103:14–22. https://doi.org/10.1016/S0924-0136(00)00413-1
16. Hughes T (1980) Generalization of Selective Integration Procedures to Anisotropic and Nonlinear Media. Int J Numer Methods Eng 15:1413–1418. https://doi.org/10.1002/nme.1620150914